

Heat pumps to upgrade existing CHP-DHN systems towards new generation thermal networks

A. Mugnini^{a,*}, G. Comodi^a, A. Arteconi^{a,b}

^a Dipartimento di Ingegneria Industriale e Scienze Matematiche, Università Politecnica delle Marche, Via Brecce Bianche 12, Ancona 60131, Italy

^b Department of Mechanical Engineering, KU Leuven, Leuven B-3000, Belgium

ARTICLE INFO

Keywords:

District heating network
Combined heat and power
Heat pump
Upgrade of 3rd generation DHN
Sustainability

ABSTRACT

District heating networks with combined heat and power systems and renewable energies are one of the most promising solutions for efficient and sustainable energy supply. In many cases, however, especially for district heating networks prior to the 4th generation, significant renovations are required to meet decarbonization targets. In this paper a study is proposed to evaluate the integration of high temperature heat pumps in an existing combined heat and power - district heating plant to reduce fossil fuel consumption and increase the exploitation of renewable energy sources. The plant is currently operating in central Italy and connects more than 1250 users. The identified solution implies lowering the district heating networks operating temperature and supplying power peaks with a high temperature heat pump acting as a booster. Results showed significant improvements in system performance especially in the winter months, due to the greater impact of lowering the temperature level of the district heating network during these months. Overall, the updated scenario allows the overall demand and ground heat losses to be reduced annually by 5.3 % and 13.5 % respectively. This reduces natural gas consumption by 13.3 % and avoids the emission of about 836 tCO₂. The analysis provides guidelines for the upgrade of 3rd generation district heating network that can be useful for planning improvements towards newest generation thermal networks.

1. Introduction

According to the International Energy Agency, buildings are responsible for about 30 % of total energy demand and about 28 % of climate-changing gas emissions (International Energy Agency (IEA), 2023). One of the most energy-intensive requirements in buildings is meeting the demand for space heating and cooling (González-Torres et al., 2022). Considering space heating, it is estimated that about two-thirds of requirements are still met by fossil fuels (International Energy Agency (IEA), 2023). In addition, individual generators (such as traditional natural gas boilers) are mostly widespread (International Energy Agency (IEA), 2023).

District Heating Networks (DHNs) represent one of the most interesting solutions to achieve decarbonization of the building heating sector (International Energy Agency (IEA), 2023). Indeed, many benefits can be gained from the broad deployment of DHNs. The first is the possibility of switching from individual to centralized heat generation. Centralized heat generation allows for increased efficiency and the integration of different energy sources, such as waste heat or renewable

energy sources (Angelidis et al., 2023; Zhang et al., 2022). Moreover, DHNs allow the exploitation of different levels of thermal inertia, both intrinsically available in the network and provided by the integration of a dedicated Thermal Energy Storage (TES) (Vandermeulen et al., 2018). This can greatly help the management of the entire energy system, especially when high penetration of non-programmable renewable sources is expected.

Despite the countless benefits that can be achieved, DHNs are not yet widely widespread. In fact, according to 2021 data, only 8 % of the global heat demand (considering both buildings and industries) is satisfied by DHNs (International Energy Agency (IEA), 2023) of which 90 % is still obtained from fossil sources (International Energy Agency (IEA), 2023). In recent times, solutions to identify completely sustainable and manageable DHNs have become increasingly popular. A new concept of new generation DHNs is in fact emerging (Guo et al., 2024), these are called 4th (Kallert et al., 2021; Jodeiri et al., 2022) and 5th (Volkova et al., 2022; Abugabbara et al., 2023) generation DHNs. 4th and the 5th generation networks provide for low-temperature operation (i.e., 30°C–60°C for 4th generation DHNs and lower than 45°C for 5th generation (Guo et al., 2024)) to reduce heat losses and allow the use of

* Corresponding author.

E-mail addresses: a.mugnini@univpm.it (A. Mugnini), g.comodi@univpm.it (G. Comodi), a.arteconi@univpm.it (A. Arteconi).

Nomenclature		\dot{Q}	Heat power (Wth)
<i>Acronyms</i>		t	Time (s)
C	Commercial users	T	Temperature (°C)
CHP	Combined Heat and Power	U	Total equivalent loss coefficient of piping by unit length (W K ⁻¹ m ⁻¹)
DHN	District Heating Network	η	Efficiency (-)
HTHP	High Temperature Heat Pump	<i>Subscripts</i>	
NG	Natural Gas	boiler	Referred to natural gas boilers
PV	Photovoltaic Plant	chp	Referred to combined heat and power
PID	Proportional-Integral-Derivative	dhw	Referred to domestic hot water
R	Residential users	el	Referred to electrical efficiency
TES	Thermal Energy Storage	env	Referred to the environment in which the pipes are placed
<i>Symbols</i>		in	Referred to an input quantity
COP	Coefficient of Performance (-)	indoor	Referred to indoor air temperature
ctrl	Control signal (-)	out	Referred to an output quantity
cp	Specific heat (J kg ⁻¹ K ⁻¹)	outdoor	Referred to outdoor air temperature
l	Length (m)	sh	Referred to space heating
L	Thermal losses coefficient (Wth K ⁻¹)	th	Referred to thermal efficiency
M	Mass (kg)	u	Referred to the general group of users
\dot{m}	Flow rate (kg s ⁻¹)		

low-temperature heat generation technologies such as heat pumps (Gong et al., 2023).

Considering the European case, there are still very few DHNs in operation that can be considered 4th or even 5th generation, but on the contrary, most systems are old and inefficient (European Commission). Therefore, in addition to promoting the increasingly large-scale deployment of new-generation DHNs, a good contribution towards decarbonization goals can be made by upgrading existing networks, especially those prior to the 4th generation.

The oldest DHNs, i.e., 1st, 2nd and 3rd generation DHNs (Mazhar et al., 2018), could be renovated with various interventions. For example, strategies can be adopted to reduce heat loss to the ground (Merlet and Baviere, 2023). In this respect, Jing et al. (Jing et al., 2023) showed the effect of renovating old pipes. In particular, Jing et al. showed that by using cured-in-place pipe liners, losses can be reduced by up to 55.4 %. Another way to reduce losses is to lower as much as possible the supply temperature (Mugnini et al., 2021). In this regards Capone et al. (2023) pointed out that, considering the Italian case study, around 10 % of existing networks do not actually require supply temperatures above 90°C. Capone et al. also showed how a supply temperature of 90°C can be achieved, compatibly with operational constraints, by the most of existing Italian DHNs, which currently operate at higher temperature levels. The benefits of such this strategy are proven by several studies. For instance, according to Nord et al. (Nord et al., 2018), reduction in thermal losses up to 25 % can be reached lowering the water supply temperature, while Østergaard and Svendsen achieved reductions of up to 35 % (Østergaard and Svendsen, 2018). Another strategy to upgrade existing DHNs is to replace heat generators with more sustainable technologies or to exploit multiple energy carriers available. In this regard, Comodi et al. (2017) assessed an improvement in primary energy saving if a Combined Heat and Power (CHP) is included in the generation system of an existing DHN feed with traditional natural gas boilers. On the other hand, Shabanpour-Haghighi and Seifi (2016) demonstrated the improved performance in terms of both primary energy and cost savings when a multi-energy system is exploited in a DHN. On this subject, another interesting study is the one proposed by Fu et al. (Fu et al., 2021). Fu et al. estimated that, exploiting a multi-energy system in which one source is given by low-quality waste heat from power plants and industrial plants in China to fuel DHN, consumption and emissions can be reduced by up to 80 % compared to coal-fired boilers. Alternatively, to increase the performance of existing

DHNs, advanced control techniques (i.e., model predictive control or reinforcement learning) can be used to exploit the thermal inertia available in the network (Mugnini et al., 2022). In this way, different objectives (e.g., total costs or energy consumption) could be pursued. For instance, Verrilli et al. (2017) calculated a potential cost reduction of 7.5 % if a model predictive control is implemented to optimally manage the operating heat generation system of a DHNs. Also Hassan et al. (Hassan et al., 2023) demonstrated the benefits of optimal control over the energy performance of a DHN network. In particular, Hassan et al. showed how optimised scheduling of the water flowrates in the DHN over several days allows a cost reduction of up to 21 % when DHN can exploit a dedicated TES. Li et al. (2023), instead, showed how a model predictive control can reduce the heat energy consumption of a DHN by up to 7.4 % while also improving the internal temperature stability in rooms.

These are just a few examples of studies demonstrating the benefits of multiple strategies for improving existing 1st, 2nd and 3rd generation DHNs. However, in recent times interest is also growing in another intervention involving the integration of High Temperature Heat Pumps (HTHPs) in DHNs (Hamid et al., 2023). HTHPs work with a sink temperature ranging from 90°C to 160°C and have typically been used in the industrial sector (Arpagaus et al., 2018). In fact, the idea of using HTHP in existing DHNs brings countless advantages, including the possibility of increasing the share of heat and electricity generated from renewable energy sources and providing more flexibility to the grid by using the inertia of the grid (Barco-Burgos et al., 2022). Some studies are beginning to investigate the integration of HTHPs, especially in existing networks. For instance, Ommen et al. (Ommen et al., 2015; Ommen et al., 2014) evaluated the operational performance of different plant configurations in which a HTHP is optimally integrated into a DHN. Mateu-Royo et al. (Mateu-Royo et al., 2020) showed that the integration of a HTHP into a district heating network operating in Sweden results in CO₂ emission savings of around 60 % compared to the original generation mix. Even according to Ochs et al. (Ochs et al., 2022), savings in CO₂ emissions in the order of 63 % can be estimated if HTHPs are integrated into typical DHNs systems (with a significant fossil share) and considering the current European electricity mix.

Although, as in the above examples, the application of HTHPs to DHNs as a renewal solution is now much discussed in the literature, there are not many examples available in which the practical benefits are demonstrated in operating DHNs. This work fits into this context. In

fact, the innovative aspect of this study is to propose an evaluation of the actual energy performance that the addition of a HTHP to the heat generation system of an existing 3rd generation DHN can have. This study aims to provide a practical example of retrofitting an existing DHN-heating system. Based on dynamic simulation models trained with measured data of the real system, a quantitative energy analysis is presented to evaluate the performance improvements that can be achieved with the proposed upgrading strategy. The study discusses practical aspects that can be helpful in understanding pros and cons of HTHP integration in the district.

The DHN analyzed is currently in operation in Osimo (central Italy) and the analysis deals with the assessment of the impact on consumption and emissions of a management strategy that includes the lowering of the water operating temperatures and the addition of an HTHP as a booster. At present, the DHN is powered by a power plant consisting of CHP and Natural Gas (NG) boilers (Mugnini et al., 2021). Furthermore, a Photovoltaic (PV) Plant is also present in the installation and the energy analysis will evaluate the possible increase in PV electricity self-consumption resulting from the operation of the booster.

It is important to point out that the analysis presented in this study is highly dependent on the architecture of the DHN considered and the operational constraints of the real system. However, since the study is carried out on real data, the intent is to present a scenario that can be useful for planning improvements towards newest generation thermal networks.

The structure of this paper is organized as follows. Section 2 describes the methodology. Since modelling is closely linked to the specific case study, Section 2 contains both the description of the case study and the models. Section 3 describes the results of the energy analysis and, finally, Section 4 summarizes the most relevant conclusions of the study.

2. Methodology

This section describes the methodology used to realize the energy analysis. To make the understanding of the methodology clearer, a brief description of the case study will be given in the first subsection (subsection 2.1). Therefore, the second subsection outlines the main features of the model used to simulate the dynamics of the DHN and its heat generation plant and the HP (subsection 2.2). Finally, the last subsection contains a description of the performance indicators used to evaluate the renovation intervention (subsection 2.3).

2.1. Description of the case study

This section contains the description of the case study considering both the current operation scenario and the upgraded scenario. The next three subsections briefly describe the main characteristics of the DHN, the CHP and the current plant operation strategy. More details about the case study can be retrieved in the previous works (Mugnini et al., 2021; Corradi et al., 2021).

2.1.1. District heating network

In this study, a real DHN network currently operating in Central Italy (Osimo, 43°29' N, 13°29' E) is analysed. The network connects about 1278 utilities, both residential and public/commercial. Residential users require about 49 % of the total heat demand carried by the network, while the remaining demand is due to public/commercial end-users. The network has a length of about 45 km and contains a total volume of water of about 444 m³. The pipes are insulated with polyurethane and have an external mechanic protection in polyethylene.

The DHN is made up of two main circuits: the first circuit is directly connected to the thermal power plant and supplies heat to end users located at altitudes between 90 and 190 m above sea level, while the secondary circuit is disconnected from the primary one through two plate exchangers located in a pumping station and serves users located between 180 and 255 m above sea level.

Fig. 1(a) shows the heat power demand satisfied by the DHN (real data measured for the year 2018). Peak demand is around 9.13 MW_{th} and takes place in January, while in summer the demand drops significantly to a base value of 2 MW_{th}. Fig. 1(b) also shows the trend of the outdoor air temperature measured in Osimo (Ancona, Italy) near the thermoelectric power plant.

2.1.2. Combined heat and power

In the current configuration, the DHN is heated by a heat generator composed of a CHP plant and two operating boilers. The CHP is a NG fuelled internal combustion engine (rated heating power of 1.3 MW_{th} and 1.2 MW_{el} of rated electrical power, thermal efficiency of 42 % and electrical efficiency of 41 %). The two boilers, each with a power of rated heating power of 4.6 MW_{th} and an efficiency of 96 %, are also envisaged to satisfy the heat demand when the demand exceeds the CHP capacity. Fig. 2 shows a schematic of the heat generator current in operation.

2.1.3. Current DHN-CHP plant management

Two levels of CHP-DHN plant management can be distinguished. The first concerns the CHP plant management. The choice of the heat generation unit varies depending on the season and aims to prevent the CHP working for too long at a modulation less than 60 %. In winter (November–March), the CHP is always operating and the boilers serve as integration. The CHP is switched off during the night (from 8.00 pm to 7.00 am) in mid-season (April–mid-June and mid-September–October). In mid-season overnight demand is covered only by boilers, while daytime operation is the same as winter. Finally, during summer (mid-June–mid-September), the CHP is always switched off and only boilers are active. As for the second level of management, this is referred to the regulation of DHN. A PID (Proportional-Integral-Derivative) control is used to regulate the flowrate to maintain the water supply temperature value and the desired pressure in the circuit. Currently the following seasonal supply temperature value are selected: 95 °C in winter, between 78°C and 85°C in mid-season and 75 °C in summer. These temperature levels are chosen in line with the operational constraints, i.e., the maximum flow rate of the hydraulic pump (i.e., 250 m³/hr), health reasons (e.g., avoid legionella) and the peak demand of users.

With this network management strategy, the heat losses towards the ground are quite high. Table 1 shows the estimated thermal losses to the soil for each month based on the measured data (Comodi et al., 2017). It can be noted that thermal losses account for about the 20 % of the total heat demand in winter. This percentage reaches 63 % in summer.

2.1.4. Upgrade of DHN-CHP plant

The intervention to upgrade the existing DHN-CHP system consists of introducing a HTHP as a booster to the existing CHP plant. The aim is to lower the DHN operating temperatures to the lowest allowable value to avoid legionella problems (70–75 °C). In this way the HTHP is switched on only to chase the peaks of the heat demand.

The upgraded CHP plant configuration is shown in Fig. 3, in accordance with the suggestions of Barco-Burgos et al. (Barco-Burgos et al., 2022). The return line is used as heat source to evaporate the refrigerant while the supply line is heated by the HTHP condenser. Thus, the HTHP works as a booster downstream of the current CHP plant. The HTHP compressor is supplied by electricity from the grid. In the case study analysed, however, there is also the possibility of exploiting the excess generation of an extensive PV plant serving the city of Osimo. The objective of the intervention is therefore twofold: (i) to reduce heat losses to the soil and (ii) to increase the self-consumption of renewable energy available.

2.2. Modelling of the case study

In this section the models to simulate the above case studio are described, both in the current configuration and in the updated

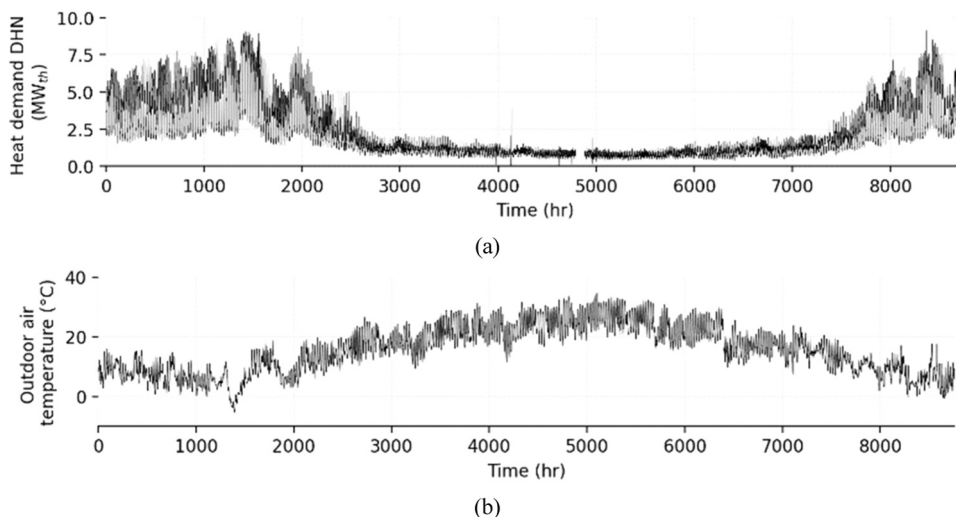


Fig. 1. (a) Yearly heat power demand satisfied by the DHN and (b) outdoor air temperature (real data measured, year 2018).

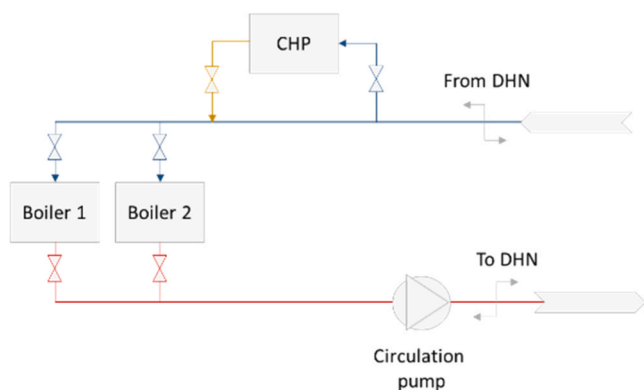


Fig. 2. Scheme of the heat generation currently in operation.

Table 1
Heat losses compared to monthly heat demand (year 2018).

Month	Heat demand (GWh _{th})	Heat losses (GWh _{th})
January	3.10	0.62
February	3.44	0.61
March	3.12	0.68
April	1.33	0.53
May	0.87	0.46
June	0.69	0.41
July	0.60	0.38
August	0.57	0.36
September	0.67	0.39
October	0.89	0.45
November	1.95	0.51
December	3.25	0.59

configuration. The final sub-section also shows the main key performance indicators for the energy analysis reported in the results.

2.2.1. DHN-CHP modelling

The energy analysis is carried out through the results obtained with a dynamic model of the system validated with real data. The model has been extensively described in (Mugnini et al., 2021). However, to make the understanding of energy analysis clearer, the modelling technique is also described in detail in this subsection. Two key parts can be distinguished: the first concerns the modelling of the DHN and the other the thermal generation system (CHP system).

The DHN is modelled using a mixed approach (i.e., white-box and black-box models) in relation to available plant data. In particular, the thermal model of the pipelines is carried out using a purely physical approach, while user demand is modelled with linear equations that allow for the dependence of demand on outdoor air temperature and internal user setpoint. In the latter case, the equations are calibrated based on available data.

Since the purposes of this study concern the evaluation of the thermal power plant-side convenience of the upgrade strategy, the DHN model involves only energy balances. Hydraulic contributions related to pressure drops are excluded for the purposes of the objectives of this analysis. Furthermore, individual users connected to the network were not individually modelled in detail. The heat demand side was then modelled by introducing 5 macro-users connected to the network. The impact on the aggregate thermal demand of individual macro-users was assessed in relation to known real system characteristics and only available aggregate thermal demand data. Specifically, the following measured data are available: overall volumetric flowrate and operating temperatures (DHN supply and return temperatures).

The 5 macro-users modelled are divided as follows: 4 macro-users are representative of residential (R1, R2, R3, R4) building clusters, while 1 represents commercial (C) buildings. Fig. 4 shows the macro-users in the different branches of the network.

In relation to the characteristics of the real system, the commercial macro-user (C) account for 47 % of the total heat demand, while the residential macro-users (R1, R2, R3 and R4) represent the remaining 53 %. Based on calibration with available aggregate heat demand data, the following weights are assigned to the single residential macro-users: 5.3 % for R1, 18.5 % for R2, 18.5 % for R3 and 10.6 % for R4.

The total heat demand of each macro-user (\dot{Q}) is due to both space heating of each macro-users (\dot{Q}_{shu}) and domestic hot water (\dot{Q}_{dhw}), as shown in Eq. (1).

$$\dot{Q} = \dot{Q}_{dhw} + \sum_{u=1}^5 (\dot{Q}_{shu}) \tag{1}$$

The heat demand for space heating of each macro-user (\dot{Q}_{shu}) is obtained according to Eq. (2), where $T_{indooru}$ and $T_{outdoor}$ are respectively the outdoor air temperature and indoor air temperature setpoint (assumed to be the constant value of 20 °C to ensure comfort), L_u represents the global coefficient of heat loss to the outside of the macro-user and $ctrl_u$ the control signal for the heating demand of macro-user (1 on, 0 off).

$$\dot{Q}_{shu} = L_u \cdot ctrl_u \cdot (T_{indooru} - T_{outdoor}) \tag{2}$$

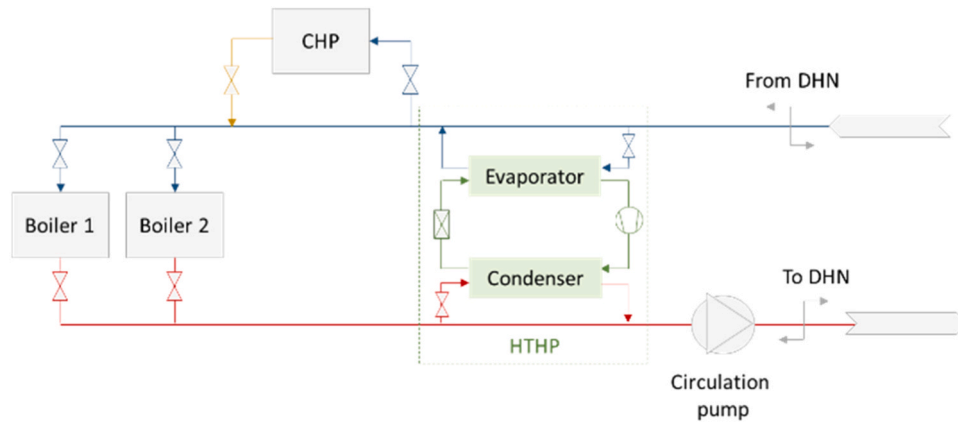


Fig. 3. Scheme of the upgrade of CHP-DHN plant.

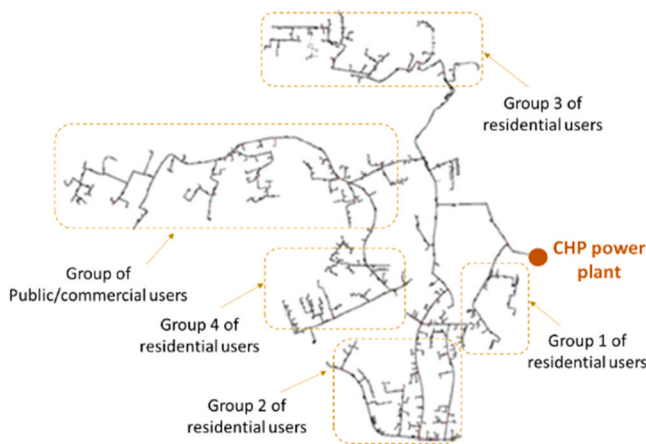


Fig. 4. DHN layout and clusters of users identified for modelling the network (Mugnini et al., 2021).

L_u values were obtained through calibration of the model with the measured data. In particular, Table 2 summarizes the values obtained.

To represent diversified heat demand, different occupancy profiles (modelled with $ctrl_u$) were considered for residential and commercial macro-users. Specifically, 3 profiles (i.e., A, B, and C) were introduced for residential users and 2 profiles (i.e., A and B) for commercial users. These were chosen based on the information available for end users and were applied uniformly throughout the space heating season (i.e., from the 1st of November to the 15th of April, duration of the heating season for Osimo, Italy). The occupancy profiles are shown in Figs. 5 and 6. In addition, Table 3 also shows the daily schedule for each user. Considering the types of residential occupants, profile A is typical of users who are unemployed or work from home, profile B is typical of working users who return home for lunch, and profile C is representative of working users who do not return home for lunch. On the other hand, with regard to commercial users, types A and B respectively distinguish businesses that are not open for lunch from those that are open all day.

Table 2
 L_u -values for the single groups users (Mugnini et al., 2021).

Group of user	L_u (kW _{th} K ⁻¹)
R1	21.2
R2	74.4
R3	74.4
R4	42.0
C	188

Each residential macro-user is assumed composed of 50 % users of type A (Fig. 5a), 25 % of type B (Fig. 5b) and 25 % of type C (Fig. 5c). Fig. 7 makes explicit the overall values of the L_u coefficient for individual macro-users (Table 2) and occupancy profiles (Figs. 5 and 6). Regarding the commercial macro-user: 50 % of the users are of type A (Fig. 6a) while the remaining 50 % is of B (Fig. 6b).

Regarding domestic hot water demand (\dot{Q}_{dhw}), the authors assumed a heat demand profile by analyzing the base load from the aggregate measured data. In particular, it was assumed that the heat demand for domestic hot water coincides with the base load of the aggregate demand. So from the observation of aggregate heat demand, an overall demand profile was deduced for domestic hot water (\dot{Q}_{dhw} in Fig. 8), which is then allocated to the various macro-users according to their percentages of influence on the overall demand.

Fig. 9 shows the outline of the DHN as modelled. To distribute the flowrate among the macro-users, the thermal demand split percentages (i.e., 5.3 % for R1, 18.5 % for R2, 18.5 % for R3 and 10.6 % for R4) are used. Pipe diameters are estimated to keep the fluid velocity between 1 and 1.5 m s⁻¹ based on commercial pipe diameters, according to the methodology described in (Mugnini et al., 2021). As for the length of the pipes of the various branches, this was chosen to obtain the same total fluid volume content as the real DHN (i.e., 444 m³).

As concern the model of the pipes in the DHN, it is realized with a “plug-flow” model (Solar Energy Laboratory). In particular, the single pipe is divided into fluid segments of variable size. The fluid entering at a given timestep physically displaces the position of the various segments within the pipeline (the following simplified assumptions are made: (i) the segments are immiscible and (ii) there is no conductive heat exchange between adjacent segments). According to this model, the mass of fluid (M_{in}) entering the pipeline is given by:

$$M_{in} = \dot{m}_{in} \Delta t \quad (3)$$

Where \dot{m}_{in} is the input flow rate (in kg s⁻¹), t represents the time passing in the simulation and Δt the timestep (both in s). According to ratio of the input mass to the total mass contained in the pipe (M), the “plug-flow” model defines a different set of equations. In addition, Fig. 10 summarizes the pipeline modelling according to the “plug-flow” model. If M_{in} is greater than M , first the heat losses to the external environment are calculated (as if all the mass entering Δt exchanged with the external environment, dividing the time the mass stays inside the tube into time intervals). The discretized energy balance is:

$$\dot{m}_{in} \Delta t c_p \frac{T_{in}(t+1) - T_{in}(t)}{\Delta t} = U l (T_{env}(t) - T_{in}(t)) \quad (4)$$

Where U is a total equivalent loss coefficient by unit length (in W K⁻¹), l is the pipe length (in m), T_{env} is the temperature of the environment in which the pipes are placed and c_p is the specific heat of the fluid (in J

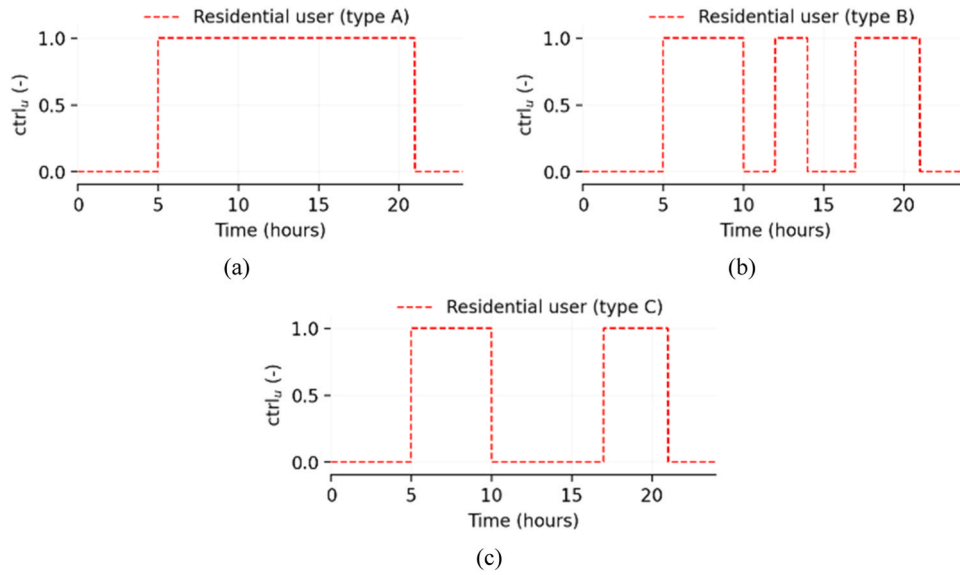


Fig. 5. $ctrl_u$ trend for different types of residential users.

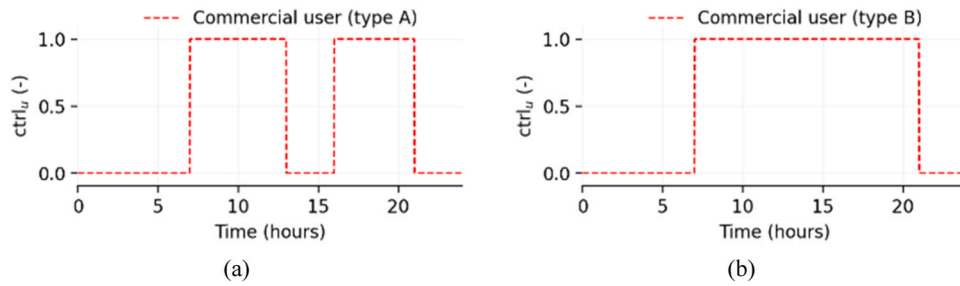


Fig. 6. $ctrl_u$ trend for different types of commercial users.

Table 3
period of occupation for each type of user.

Type of user	Period of occupation ($ctrl_u$ equal to 1)
Residential user type A	From 5.00 am to 9.00 pm
Residential user type B	From 5.00–10.00 am, from 12.00 pm to 2.00 pm and from 5.00 pm to 9.00 pm
Residential user type C	From 5.00–10.00 am and from 5.00 pm to 9.00 pm
Commercial user type A	From 7.00 am to 1.00 pm and from 6.00 pm to 9.00 pm
Commercial user type B	From 7.00 am to 9.00 pm

$kg^{-1} K^{-1}$). On the other hand, when M_{in} is lower than M , first, mass displacement is solved and then heat transfer. Referring to Fig. 10, the outlet temperature (T_{out}) is calculated according to Eq. (5).

$$T_{out} = \frac{M_3 T_3 + (M_{in} - M) \bullet T_2}{M_{in}} \quad (5)$$

Then, the heat exchange is evaluated individually for each internal block (Eq. (6)).

$$M_i c_p \frac{T_{in,i}(t+1) - T_{in,i}(t)}{\Delta t} = U_i (T_{env}(t) - T_{in,i}(t)) \quad (6)$$

In general, thermal losses to the ground are calculated assuming a total equivalent loss coefficient for the pipes (U) equal to $0.68 W m K^{-1}$ (Mugnini et al., 2021). Thus, by adding up the heat losses to the ground of each branch in Fig. 9, it is possible to obtain the value of total losses

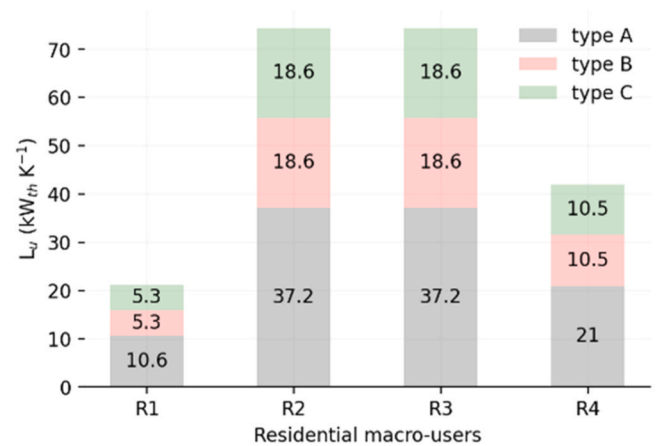


Fig. 7. L_u -values ($kW_{th} K^{-1}$) for the single residential macro-users.

(\dot{Q}_{loss}). Consequently, the total heat output to be covered by the heat generator is given by the sum of the losses to the ground (\dot{Q}_{loss}) and the heat demand of the users (\dot{Q}).

As for the CHP plant model, the variation of the heat generator performance (i.e., CHP and boilers) with the operating conditions (i.e., outdoor air temperature and modulation degree for CHP and modulation for boilers) are obtained through the training of a polynomial black box model with the measured data (Mugnini et al., 2021). Such polynomial equations are described by Eqs. (7)–(10). In particular, Eq. (7)

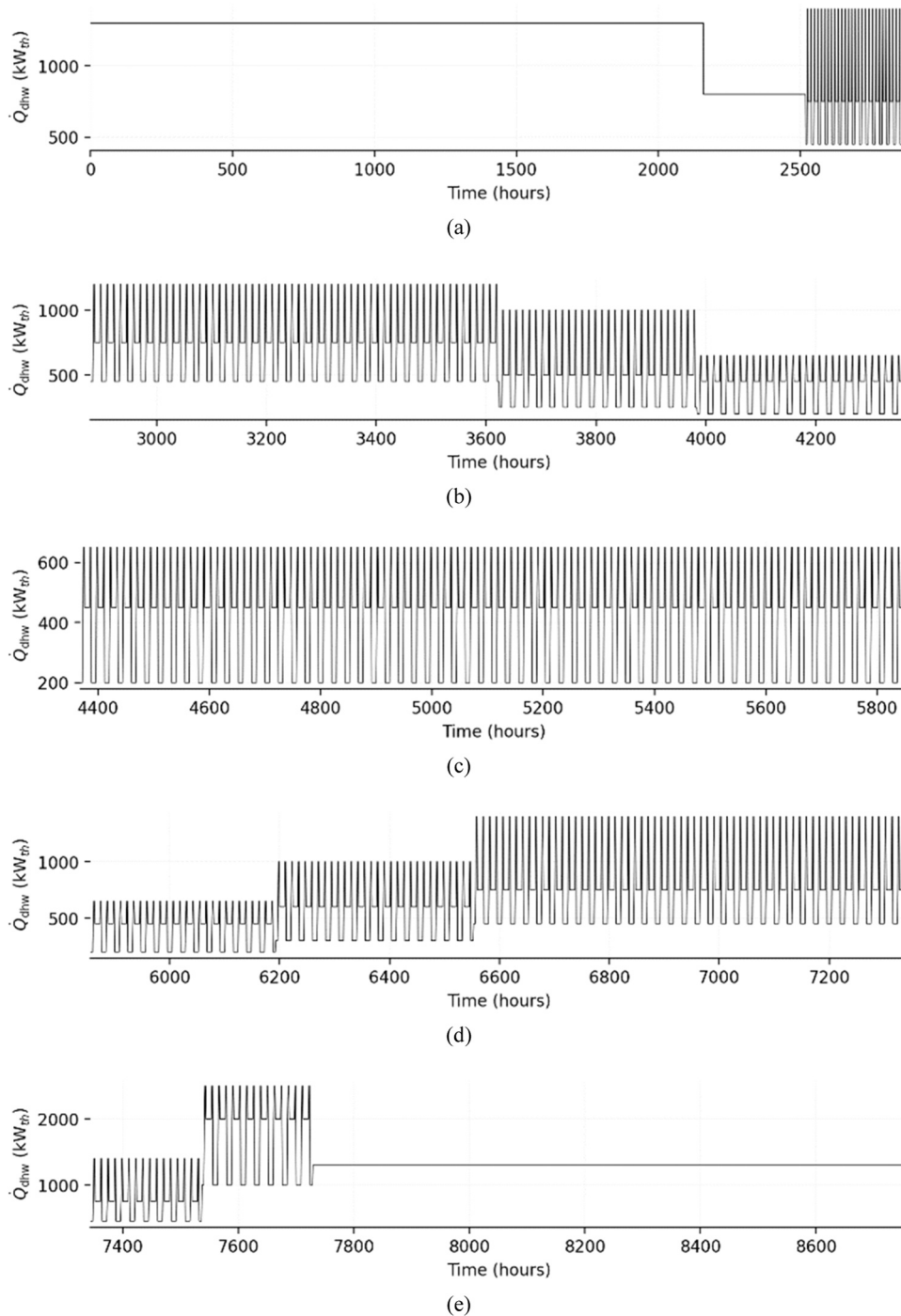


Fig. 8. \dot{Q}_{dhw} trend over the year: (a) from January to April; (b) from May to June; (c) from July to August; (d) from September to October and (e) from November to December.

allows obtaining the thermal efficiency of the CHP ($\eta_{th, chp}$) as a function of the heat output satisfied by the CHP (\dot{Q}_{chp}) and the outdoor air temperature ($T_{outdoor}$). Eq. (8) allows obtaining the electrical efficiency of the CHP ($\eta_{el, chp}$) as a function of electrical power produced by the CHP (\dot{P}_{chp}) and the outdoor air temperature ($T_{outdoor}$). Eq. (9) makes it possible to correlate the electric power produced (\dot{P}_{chp}) with the thermal power met by the CHP (\dot{Q}_{chp}). Finally, Eq. (10) allows the efficiency of each boiler ($\eta_{th, boiler}$) to be evaluated as a function of the heat output satisfied by each boiler (\dot{Q}_{boiler}).

$$\eta_{th, chp} = -0.01066 + 0.008915 \cdot \dot{Q}_{chp} + 0.001183 \cdot T_{outdoor} - 4.544 \cdot 10^{-5} \cdot (\dot{Q}_{chp})^2 - 7.05 \cdot 10^{-6} \cdot \dot{Q}_{chp} \cdot T_{outdoor} - 2.803 \cdot 10^{-5} \cdot (T_{outdoor})^2 \quad (7)$$

$$\eta_{el, chp} = -6.81295 \cdot 10^{-4} + 0.00956 \cdot \dot{P}_{chp} + 6.39961 \cdot 10^{-5} \cdot T_{outdoor} - 5.5346 \cdot 10^{-5} \cdot (\dot{P}_{chp})^2 - 2.4418 \cdot 10^{-6} \cdot \dot{P}_{chp} \cdot T_{outdoor} - 1.3510 \cdot 10^{-6} \cdot (T_{outdoor})^2 \quad (8)$$

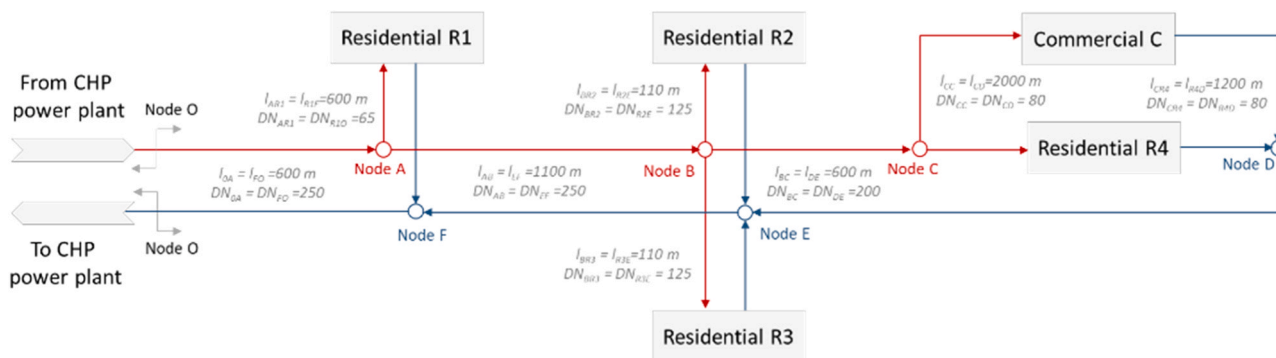


Fig. 9. Outline of the model implemented for DHN in Osimo.

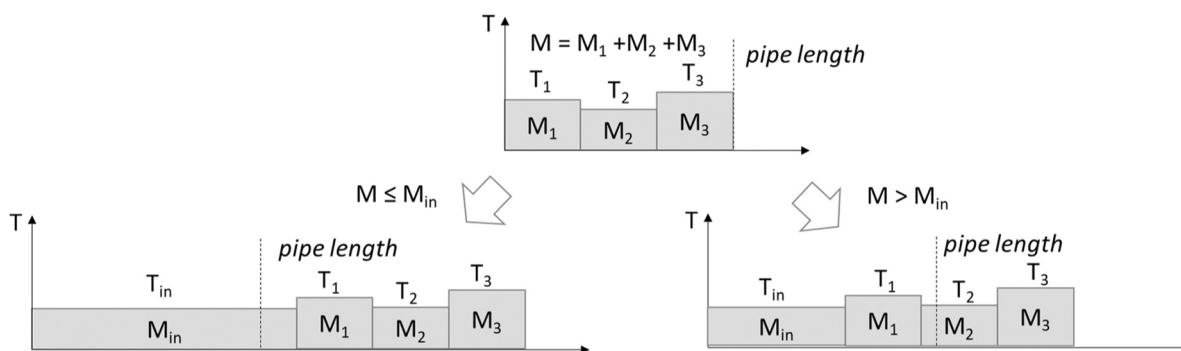


Fig. 10. Outline of the pipeline modeling (“plug-flow” model).

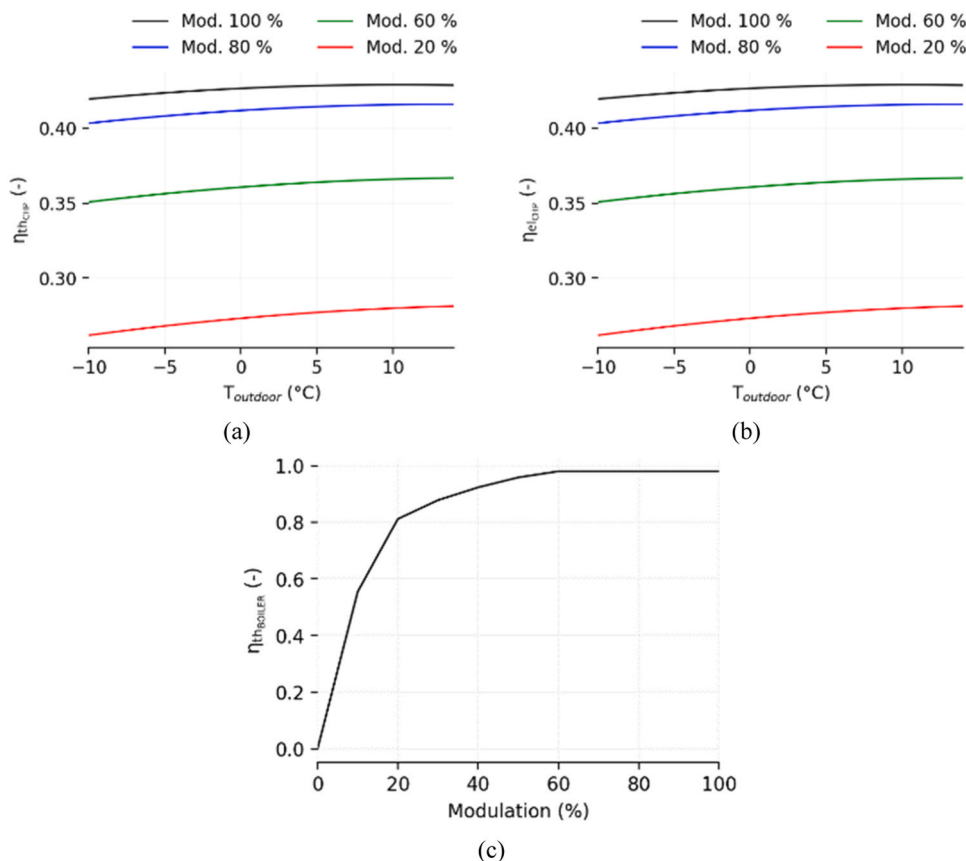


Fig. 11. Efficiency of the heat generator: (a) CHP thermal efficiency ($\eta_{th,CHP}$) at varying the outdoor temperature and modulation (Mod.); (b) CHP electrical efficiency ($\eta_{el,CHP}$) at varying the outdoor temperature and modulation (Mod.) and (c) boiler thermal efficiency ($\eta_{th,boiler}$) at varying the modulation.

$$\dot{P}_{\text{chp}} = 0.9595 \cdot \dot{Q}_{\text{chp}} + 3.3531 \tag{9}$$

$$\eta_{\text{th,boiler}} = -2.2338 \cdot 10^{-15} \cdot (\dot{Q}_{\text{boiler}})^9 + 9.8768 \cdot 10^{-13} \cdot (\dot{Q}_{\text{boiler}})^8 - 1.8452 \cdot 10^{-10} \cdot (\dot{Q}_{\text{boiler}})^7 + 1.8926 \cdot 10^{-8} \cdot (\dot{Q}_{\text{boiler}})^6 - 1.156 \cdot 10^{-6} \cdot (\dot{Q}_{\text{boiler}})^5 + 4.2365 \cdot 10^{-5} \cdot (\dot{Q}_{\text{boiler}})^4 - 8.7083 \cdot 10^{-4} \cdot (\dot{Q}_{\text{boiler}})^3 + 7.5 \cdot 10^{-3} \cdot (\dot{Q}_{\text{boiler}})^2 + 3.510 \cdot 10^{-2} \cdot \dot{Q}_{\text{boiler}} + 1.6755 \cdot 10^{-4} \tag{10}$$

Fig. 11 summarises the performance of the CHP (Fig. 11a) and the boiler (Fig. 11b) as the operative conditions change. Specifically for CHP, the operative conditions considered are outdoor temperature and modulation (Mod. In Figs. 11a and 11b)). The modulation is a continuous variable, and it is defined as the percentage ratio between the heat load at a given outdoor temperature and the maximum heat capacity of the CHP at that given outdoor temperature. Instead, considering the boiler, performance are evaluated only as a function of the modulation.

The described model was validated by comparing simulated results with available aggregate measured data. The extended validation results are reported in (Mugnini et al., 2021). In general, however, the model showed a good ability to reproduce the dynamics of CHP-DHN plants in the current scenario. In fact, the error on the monthly forecast of thermal demand is less than 10 % for all months. Even for the prediction of thermal losses to the ground, the percentage error remains below 15 %. More detailed comparisons between model predictions and measured data are also given in the Appendix.

2.2.2. HTHP modelling

Since no data are available from manufacturers regarding the variation of the performance with the source temperature of a water-to-water heat, the coefficient of performance was derived by modelling the thermodynamic cycle of the machine. In accordance with the temperature levels and refrigerants listed by Barco-Burgos (Barco-Burgos et al., 2022), a vapor compression cycle with R717 is modelled. Under reference conditions, the cycle runs between the temperatures of 75 °C and 55 °C for the hot and cold source, respectively. To evaluate the evaporation and condensation temperatures a temperature difference of 5 °C respect to the source and sink temperatures is assumed and an isentropic compression efficiency of 80 % considered. Fig. 12 shows the variation of the performance (evaluated by the Coefficient of Performance, COP) as source temperatures change.

To model the HTHP as a booster the following management strategy is applied. The setpoint supply temperature for the heat generation plant (i.e., CHP and boilers) is set at 70 °C. The regulation of the circulating

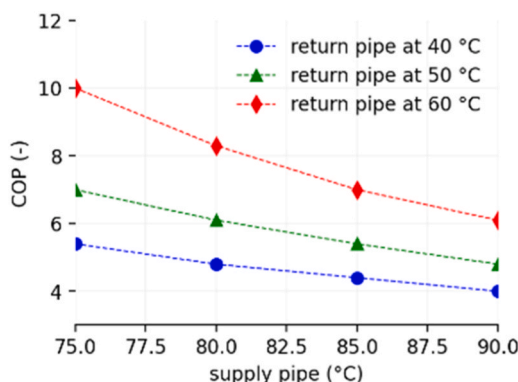


Fig. 12. Modelling of COP as the temperature of the sources varies.

flowrate keeps the return temperature in the range of 55–60 °C. When the flow rate reaches the maximum values (considered 80 % of the maximum flow, to avoid that the pump works for too long close to its operating limits), the booster is switched on and increases the supply temperature to meet the heat demand of the DHN.

2.3. Key performance indicators

The energy analysis is carried out by comparing the performance of the system in the updated case (i.e., HTHP as booster) with that obtained in the current scenario. The parameters evaluated include energy and the environmental aspects. In particular, the following monthly parameters are considered:

- Total heat demand met by the DHN.
- Thermal losses to the ground.
- Thermal demand fulfilment mode (technologies involved).
- Fuel (i.e., NG) and primary energy consumption.
- CO₂ avoided.
- Self-consumption of excess PV generation.

Specifically, the conversion factors given in (Ministero dello Sviluppo Economico (MISE), 2023) are used to estimate the primary energy consumption (1.05 for NG, 1.95 for electricity withdrawn from the grid and 1 for electricity generated from renewable sources). While (ISPRA (Istituto Superiore, 2020) is used to calculate the tons of CO₂ avoided (the assumed conversion factors are respectively 231.1 gCO₂/kWh for NG and 444.4 gCO₂/kWh for electricity withdrawn from the grid).

3. Results

This section contains the results of the energy analysis of the upgraded DHN-CHP system. The section is divided into two subsections. The first (subsection 3.1) presents, through the key performance indicators defined in the previous section, the energy analysis. Then, subsection 3.2 contains the critical discussion regarding the update of the DHN.

3.1. Energy analysis results

Fig. 13 shows the monthly heat demand that must be met by the CHP plant, distinguishing between the case of the current scenario (i.e., measured data) and the upgraded scenario (i.e., with the HTHP booster). Overall, the upgraded scenario allows an overall annual reduction in heat demand of 5.3 %. The reduction is greater in the winter months and decreases from mid-season to summer. This is because the new management strategy makes it possible a more impactful reduction of the supply temperature in winter rather than in summer when the setpoint supply temperature is already close to the allowed limit (70–75 °C for health reasons). This is even more evident by looking at the monthly distribution of DHN thermal losses to the ground (Fig. 14). Throughout the year, losses are reduced by 13.5 % and reach a peak of reduction of 18.7 % in the winter months, while the reduction is around 8 % in the summer months.

Fig. 15 shows the involvement of individual thermal generation technologies in meeting the overall heat demand. It is observed that for each month of the year the upgraded configuration does not reduce the hours of operation of the CHP and the HP only works in the winter months. Indeed, in the midseason and summer the CHP plant, already in its current configuration, is able to meet the overall demand with a discharge temperature of 70 °C. In any case, the involvement of boilers has a substantial reduction with the upgraded configuration in winter months. Indeed, throughout the year, demand covered by boilers is reduced by 25.2 %, with a peak reduction of 41.7 % in winter months.

It is important to note that, in this analysis, the maximum power of the HP is not constrained. Therefore, the study also allowed to evaluate

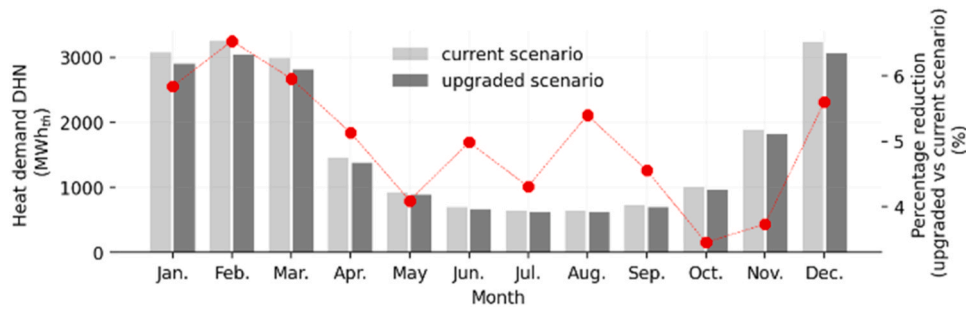


Fig. 13. Comparison of total monthly heat demand between the current scenario and the upgraded scenario.

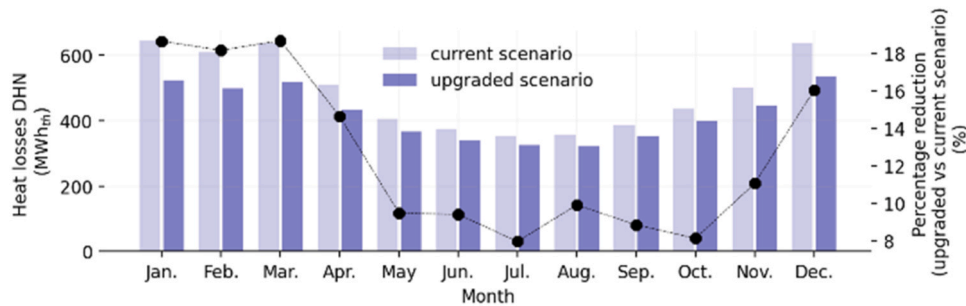


Fig. 14. Comparison of total heat losses between the current scenario and the upgraded scenario.

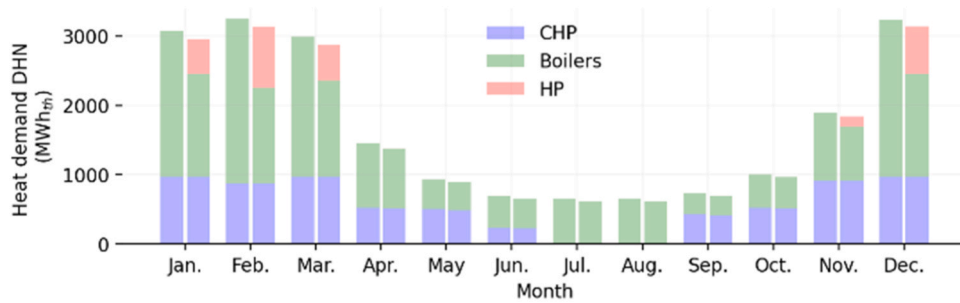


Fig. 15. Technologies involved in meeting overall demand: comparison between the current scenario and the upgraded scenario.

the size required for the HP to obtain the upgraded scenario. In particular, a peak HP power of 6.8 MW_{th} is achieved.

As regards the supply temperature reached by the HP, the maximum monthly values are generally between 72 °C and 89 °C. The maximum temperature of 95 °C is reached only once, when the peak of demand occurs (third week of February, Fig. 16 where the grey area highlights the periods when the HP is in operation).

Fig. 17 shows the comparison between the current and the upgraded scenario in terms of NG consumption (Fig. 17a) and primary energy consumption (Fig. 17b). Fig. 17c, instead, shows the comparison in

terms of CO₂ emissions between the two scenarios. The key performance indicators shown in Fig. 17 confirm that, also from an environmental point of view, the best performance gains are observed in the winter months.

In terms of NG savings, the upgraded configuration achieves an annual saving of 13.3 %, with a peak of 23.1 % for the winter months alone. Overall, the annual primary energy saving is 11.5 %, with a value of 18.9 % in the winter months. Considering the environmental aspect, Fig. 17c shows how the upgraded scenario allows to avoid on average 148 tCO₂ monthly in winter months. The analysis allowed to estimate

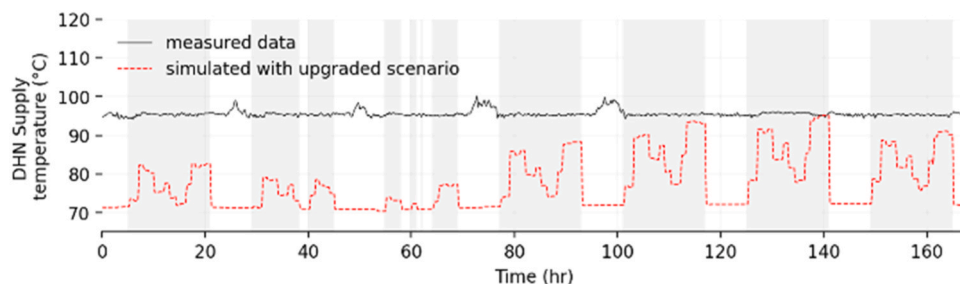


Fig. 16. DHN supply temperature comparison: measured data vs. upgraded scenario (third week of February).

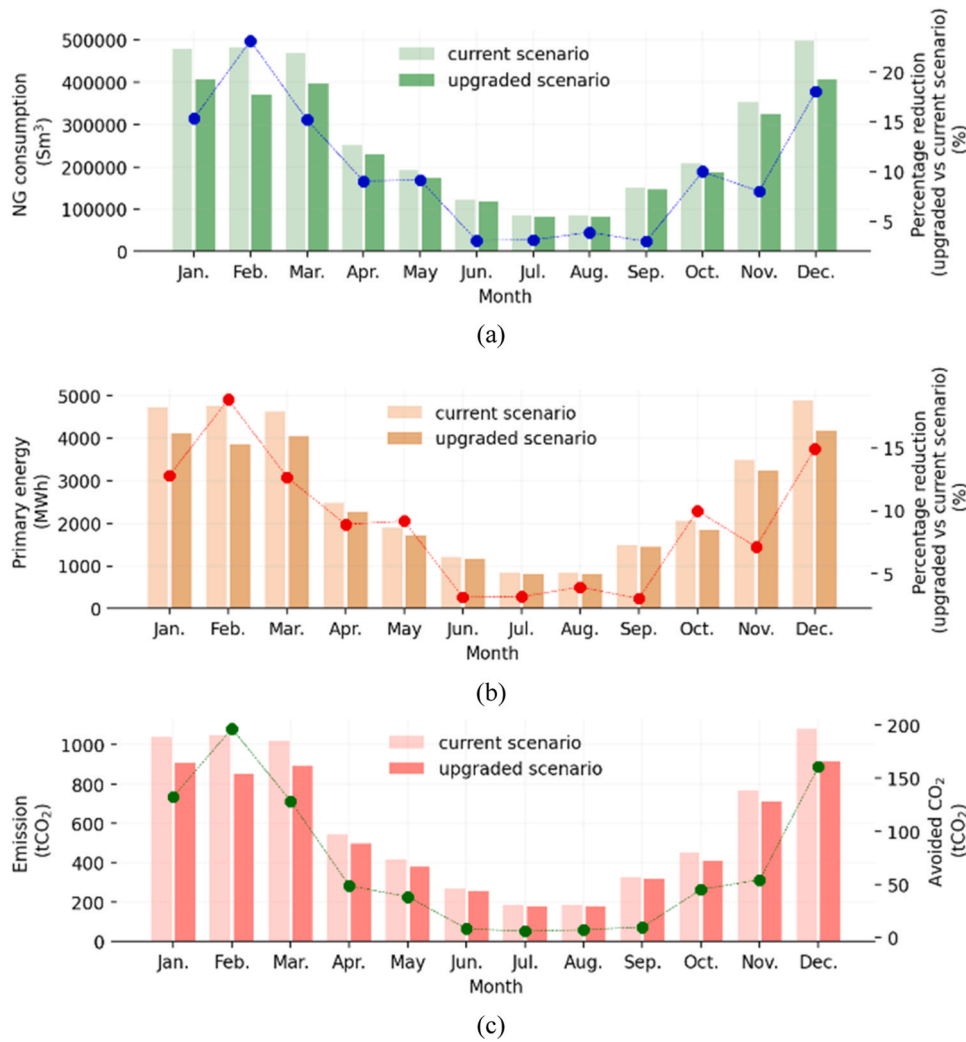


Fig. 17. Comparison between the current scenario and the upgraded scenario in terms of: (a) NG consumption, (b) primary energy consumption and (c) Avoided tCO₂ emissions.

that the use of the HTHP and the average lowering of the supply temperature allow to avoid the emission of 836 tons of CO₂ per year.

The last aspect to investigate concerns the capacity to exploit the available renewable source. Fig. 18 shows the comparison between the electrical power produced by the CHP and that consumed by the HTHP. It also highlights the electricity available as excess generation from the PV plant. Although the share of energy from renewable sources is sufficient to cover much of the HTHP demand, in the absence of a storage system to separate demand from generation, the HTHP consumption of the excess of electricity produced by the PV plant is relatively low. Indeed, the upgraded configuration allows to recover about 2.8 % of the PV excess. On the other hand, it is noted that the CHP electrical output

would be largely sufficient to drive the HTHP.

3.2. Discussion of energy analysis results

The results of the energy analysis presented in the previous section highlight some aspects concerning the proposed renovation strategy for the described Italian 3rd generation DHN. Firstly, the analysis showed that a greater impact in terms of energy and environmental benefits is achieved mainly in the winter months. Table 4 summarises the percentage variation (i.e., updated scenario versus current scenario) of the main performance indicators, distinguishing between winter, mid-season and summer season. For each indicator (excluding the

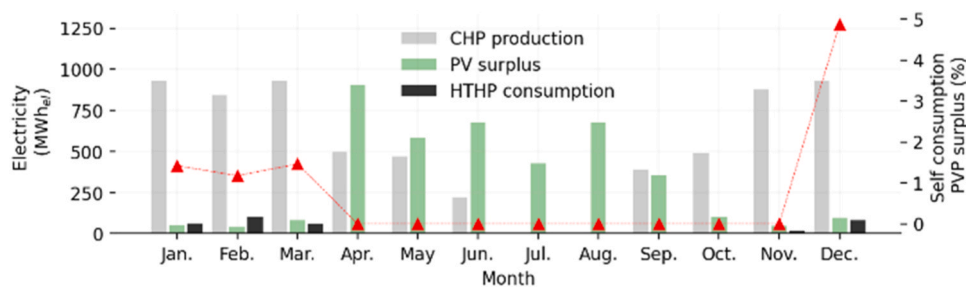


Fig. 18. Comparison between electricity produced monthly by CHP, required by HP and self-consumed by PV excess for HP (upgraded scenario).

Table 4

Percentage variation (updated vs. current scenario) in the different seasons of the year of the main performance indicators.

Key performance indicator	Winter	Mid-season	Summer
Total heat demand	-5.70 %	-4.50 %	-4.90 %
Thermal losses	-16.8 %	-10.3 %	-8.90 %
Thermal demand covered by boilers	-33.0 %	-6.20 %	-4.90 %
Thermal demand covered by CHP	0.00 %	0.00 %	0.00 %
Natural gas consumption	-16.4 %	-7.50 %	-3.50 %
Primary energy consumption	-13.7 %	-7.50 %	-3.50 %
CO ₂ emissions	-13.6 %	-7.50 %	-3.50 %

involvement of the CHP, which does not reduce its operating hours in the updated scenario), the percentage reduction decreases in absolute value from winter months to mid-season to summer months. This is because, as already mentioned, reducing the supply temperature has a greater impact in the winter months. The average monthly supply temperature is in fact reduced by 19.7 % in the winter months (from an average temperature of 91.4 °C to 73.4 °C in the updated scenario), by 12.4 % in the mid-season months (from an average temperature of 80.1 °C to 70.2 °C) and by 4.30 % in the summer months (from an average temperature of 72.1 °C to 69 °C).

Another important aspect to consider is the impact, especially in the winter months, on the operating hours of natural gas boilers, which see their operation reduced by 33.0 % in winter. This results in a substantial reduction in CO₂ emissions (13.6 % in winter). The lesser involvement of boilers is covered by HTHP, which in winter meets about 17.6 % of the total heat demand.

In addition to the clear environmental benefits and reduction in primary energy consumption (around 13.7 % considering the summer months), the use of HTHP leads to greater differentiation of the energy carriers. In fact, the emergence of a need for electricity allows the exploitation of renewable resources, which cannot be used in the current scenario. Considering the current availability of renewable sources in the case study, however, the energy analysis has highlighted the need to provide electrical storage systems to exploit any PV availability. In fact, comparing the surplus electricity available with the HTHP electricity demand, the presence of a storage battery would allow the HTHP to be powered with minimal energy withdrawals from the electricity grid (Fig. 18): comparing the overall availability of electricity from PV with the demand from HTHP in the winter months, about the 98.7 % of the demand could be covered by the PV surpluses. Anyway, due to the lack of synchronization between supply and demand, this percentage becomes 2.80 %.

To conclude, considering the energy and environmental analysis of the proposed strategy, the proposed solution brings important benefits to the entire system, especially in the winter months, but, albeit to a lesser extent, also in other periods of the year. A preliminary economic analysis also confirms the benefits of the proposed retrofit strategy. In fact, considering a price of 200 EUR/kW_{th} (Heat Pump Centre c/o RISE, 2024) for HTHP, a natural gas cost of 0.4863 EUR/Sm³ (Statista, 2023) and the cost of electricity taken from the grid of 0.24 EUR/kWh_{el} (Statista, 2024), a payback period of 6.46 years was estimated. Therefore, according to the objectives of the study, the presented analysis demonstrated from an energy, economic and environmental point of view the impact of the proposed upgrade strategy towards the conversion of operational DHNs towards new generation systems.

4. Conclusions

This study analyses an upgrade strategy for a 3rd generation district heating network currently operating in central Italy. The strategy involves lowering operating temperatures with the use of a high-temperature heat pump as a heating booster. Although the adoption of high-temperature heat pumps is a discussed solution for renovating aged

district heating networks, this study aims to present a possible application to a real case. In fact, the scenario analysis presented is based on dynamic models trained with measured data. The considerations derived from this case have a generalization potential and can be valuable for the widespread of such retrofitting solution.

The district heating network connects more than 1250 users and is supplied with a heat power plant composed of a natural gas fuelled internal combustion engine working as combined heat and power system and two natural gas boilers. Through calibrated models with real data, the study presents an energy analysis to assess the impact of the integration of a high temperature heat pump to increase the self-consumption of renewable sources available and to reduce thermal losses to the ground. The energy analysis was conducted over the whole year and highlighted to obtain the following results:

- Due to current system management conditions and operational constraints (supply temperature cannot fall below 70–75 °C for sanitary reasons) the most noticeable benefits are observed in the winter months. In fact, in the summer months the system is already regulated with a supply temperature close to the limit.
- As a result of the introduction of the heat pump, annual reductions in thermal demand of 5.3 % are estimated with a reduction in losses to the ground of 13.5 %.
- The most noticeable impact of the upgraded configuration is on boilers operating hours. In fact, possible natural gas and primary energy savings are estimated at 13.3 % and 11.5 %, respectively, resulting in CO₂ emission avoidance of about 836 tCO₂.
- The analysis on self-consumption of excess energy from renewable sources, showed that although a significant share of renewable energy is available, in the absence of storage system, self-consumption is rather low (about 2.8 %).

Thus, the energy analysis showed the benefits achievable by applying the high-temperature heat pump to lower the operating temperature of the district heating network in Osimo. The main results listed in the points above allow to directly quantify the performance achievable with this retrofitting strategy. It is worth noting that the results are highly dependent on the characteristics and operational constraints of the real system. These characteristics and operating conditions of the real system also limit the possible configuration and mode of operation of the integrated heat pump. However, for DHN systems with similar characteristics to the one analyzed in this study, energy and economic analysis showed good performance achievable with heat pump integration. Future analyses can be conducted to investigate different ways of combining the high-temperature heat pump with the system. However, the results obtained in this study, albeit with a preliminary energy analysis, can be considered significant in promoting the deployment of high-temperature heat pumps to renovate aged district heating systems.

Declaration of Competing Interest

The authors declare that they have no known competing financial interests or personal relationships that could have appeared to influence the work reported in this paper.

Data Availability

The authors are unable or have chosen not to specify which data has been used.

Acknowledgment

The authors would like to thank Astea SpA for making available the data of the CHP-DHN plant.

Appendix

This appendix provides comparisons between the model and measured data on representative weeks of the winter, mid-season and summer period.

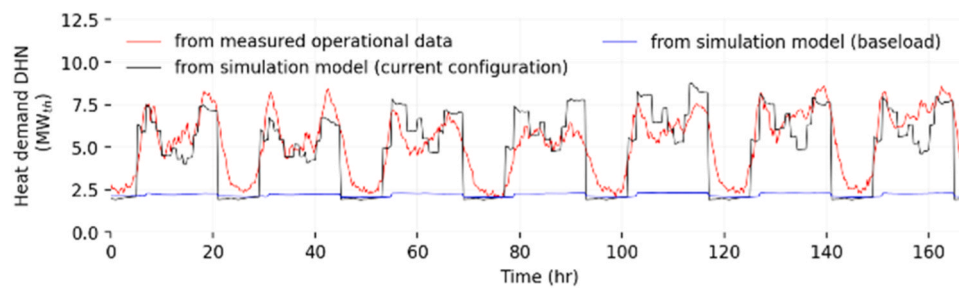


Fig. 1. A. Comparison of model and measured data for DHN heat demand and with highlighting of the modeled base load (domestic hot water and heat losses to the ground) in winter period (second week of January). Prediction error of -7.84% (the error is calculated considering only the representative period).

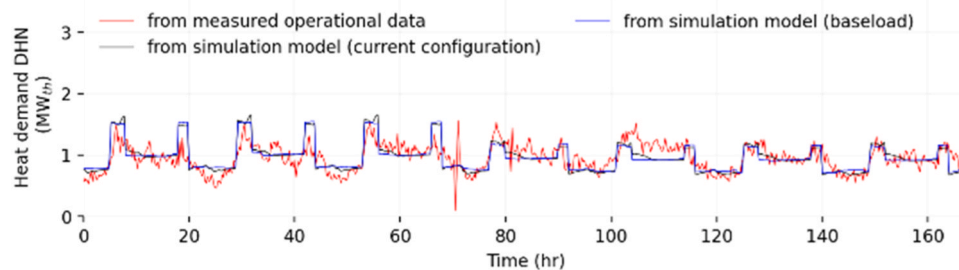


Fig. 2. A. Comparison of model and measured data for DHN heat demand and with highlighting of the modeled base load (domestic hot water and heat losses to the ground) in mid-season period (second week of May). Prediction error of 0.72% (the error is calculated considering only the representative period).

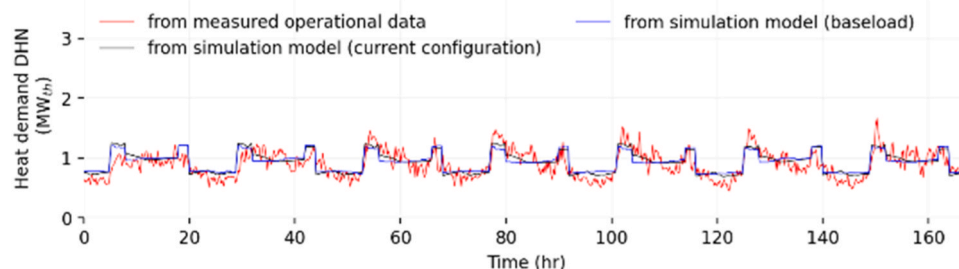


Fig. 3. A. Comparison of model and measured data for DHN heat demand and with highlighting of the modeled base load (domestic hot water and heat losses to the ground) in summer period (first week of August). Prediction error of 3.82% (the error is calculated considering only the representative period).

References

- Abugabbara, M., Gehlin, S., Lindhe, J., Axell, M., Holm, D., Johansson, H., Larsson, M., Mattsson, A., Näslund, U., Rao Puttigg, A., Berglöf, K., Claesson, J., Hofmeister, M., Janson, U., Jensen, A.W.B., Termén, J., Javed, S., 2023. How to develop fifth-generation district heating and cooling in Sweden? Application review and best practices proposed by middle agents. ISSN 2352-4847 Energy Rep. Volume 9, 4971–4983. <https://doi.org/10.1016/j.egy.2023.04.048>.
- Angelidis, O., Ioannou, A., Friedrich, D., Thomson, A., Falcone, G., 2023. District heating and cooling networks with decentralised energy substations: opportunities and barriers for holistic energy system decarbonisation. ISSN 0360-5442 Energy Volume 269, 126740. <https://doi.org/10.1016/j.energy.2023.126740>.
- Arpagaus, C., Bless, F., Uhlmann, M., Schiffmann, J., Bertsch, S.S., 2018. High temperature heat pumps: Market overview, state of the art, research status, refrigerants, and application potentials. ISSN 0360-5442 Energy Volume 152, 985–1010. <https://doi.org/10.1016/j.energy.2018.03.166>.
- Barco-Burgos, J., Bruno, J.C., Eicker, U., Saldaña-Robles, A.L., Alcántar-Camarena, V., 2022. Review on the integration of high-temperature heat pumps in district heating and cooling networks. ISSN 0360-5442 Energy Volume 239 (Part E), 122378. <https://doi.org/10.1016/j.energy.2021.122378>.
- Capone, M., Guelpa, E., Verda, V., 2023. Potential for supply temperature reduction of existing district heating substations. ISSN 0360-5442 Energy Volume 285, 128597. <https://doi.org/10.1016/j.energy.2023.128597>.
- Comodi, G., Lorenzetti, M., Salvi, D., Arteconi, A., 2017. Criticalities of district heating in Southern Europe: lesson learned from a CHP-DH in Central Italy. ISSN 1359-4311 Appl. Therm. Eng. Volume 112, 649–659. <https://doi.org/10.1016/j.applthermaleng.2016.09.149>.
- Corradi, E., Rossi, M., Mugnini, A., Nadeem, A., Comodi, G., Arteconi, A., Salvi, D., 2021. Energy, environmental, and economic analyses of a district heating (DH) network from both thermal plant and end-users' perspective: an Italian case study. Energies Vol. 12, 7783. <https://doi.org/10.3390/en14227783>.
- European Commission, CORDIS EU research results. Improving the performance of inefficient district heating networks. Available online: (https://cordis.europa.eu/programme/id/H2020_EE-02-2017/en) [Accessed: 16-November-2023].
- Fu, L., Li, Y., Wu, Y., Wang, X., Jiang, Y., 2021. Low carbon district heating in China in 2025- a district heating mode with low grade waste heat as heat source. ISSN 0360-5442 Energy Volume 230, 120765. <https://doi.org/10.1016/j.energy.2021.120765>.
- Gong, Y., Ma, G., Jiang, Y., Wang, L., 2023. Research progress on the fifth-generation district heating system based on heat pump technology. ISSN 2352-7102 J. Build. Eng. Volume 71, 106533. <https://doi.org/10.1016/j.job.2023.106533>.
- González-Torres, M., Pérez-Lombard, L., Coronel Juan, F., Maestre Ismael, R., Yan, D., 2022. A review on buildings energy information: Trends, end-uses, fuels and drivers. ISSN 2352-4847 Energy Rep. Volume 8, 626–637. <https://doi.org/10.1016/j.egy.2021.11.280>.
- Guo, Y., Wang, S., Wang, J., Zhang, T., Ma, Z., Jiang, S., 2024. Key district heating technologies for building energy flexibility: a review. ISSN 1364-0321 Renew. Sustain. Energy Rev. Volume 189 (Part B), 114017. <https://doi.org/10.1016/j.rser.2023.114017>.
- Hamid, K., Sajjad, U., Ahrens, M.U., Ren, S., Ganesan, P., Tolstorebrov, Arshad, A., Said, Z., Hafner, A., Wang, C.C., Wang, R., Eikevik, T.M., 2023. Potential evaluation of integrated high temperature heat pumps: a review of recent advances. ISSN 1359-4311 Appl. Therm. Eng. Volume 230 (Part A), 120720. <https://doi.org/10.1016/j.applthermaleng.2023.120720>.
- Hassan, M.A., Serra, S., Sochard, S., Viot, H., Marias, F., Reneaume, J.M., 2023. Optimal scheduling of energy storage in district heating networks using nonlinear programming. ISSN 0196-8904 Energy Convers. Manag. Volume 295, 117652. <https://doi.org/10.1016/j.enconman.2023.117652>.

- Heat Pump Centre c/o RISE – Research Institutes of Sweden. Annex 58. High Temperature Heat Pumps. Task Technologies Task Report ISBN 978-91-89821-34-7, Report No. HPT-AN58-2. Available online: heatpumpingtechnologies.org/annex58/wp-content/uploads/sites/70/2023/09/annex-58-task-1-technologies-task-report.pdf [Accessed: 30-April-2024].
- International Energy Agency (IEA), Space Heating, 2023. Available online: www.iea.org/reports/space-heating [Accessed: 23-November-2023].
- International Energy Agency (IEA), Buildings, 2023. Available online: www.iea.org/energy-system/buildings [Accessed: 20-November-2023].
- International Energy Agency (IEA), District Heating, 2023. Available online: www.iea.org/reports/district-heating [Accessed: 16-November-2023].
- ISPRA (Istituto Superiore per la Protezione e la Ricerca Ambientale, Italian Institute for Environmental Protection and Research), Fattori di emissione atmosferica di gas a effetto serra nel settore elettrico nazionale e nei principali Paesi Europei, 2020, (in Italian, available online) (www.isprambiente.gov.it/files2020/pubblicazioni/rapporti/Rapporto317_2020.pdf) [Accessed: 27-November-2023].
- Jing, M., Zhang, S., Fu, L., Cao, G., Wang, R., 2023. Reducing heat losses from aging district heating pipes by using cured-in-place pipe liners. *ISSN 0360-5442 Energy Volume 273*, 127260. <https://doi.org/10.1016/j.energy.2023.127260>.
- Jodeiri, A.M., Goldsworthy, M.J., Buffa, S., Cozzini, M., 2022. Role of sustainable heat sources in transition towards fourth generation district heating – a review. *Renew. Sustain. Energy Rev. Vol. 158*, 112156 <https://doi.org/10.1016/j.rser.2022.112156>.
- Kallert, A., Egelkamp, R., Bader, U., Münnich, D., Staudacher, L., Doderer, H., 2021. A multivalent supply concept: 4th Generation District Heating in Moosburg an der Isar. *ISSN 2352-4847 Energy Rep. Volume 7 (Supplement 4)*, 110–118. <https://doi.org/10.1016/j.egy.2021.09.032>.
- Li, Z., Liu, J., Jia, L., Wang, Y., 2023. Improving room temperature stability and operation efficiency using a model predictive control method for a district heating station. *ISSN 0378-7788 Energy Build. Volume 287*, 112990. <https://doi.org/10.1016/j.enbuild.2023.112990>.
- Mateu-Royo, C., Sawalha, S., Mota-Babiloni, A., Navarro-Esbri, J., 2020. High temperature heat pump integration into district heating network. *ISSN 0196-8904 Energy Convers. Manag. Volume 210*, 112719. <https://doi.org/10.1016/j.enconman.2020.112719>.
- Mazhar, A.R., Liu, S., Shukla, A., 2018. A state of art review on the district heating systems. *ISSN 1364-0321 Renew. Sustain. Energy Rev. Volume 96*, 420–439. <https://doi.org/10.1016/j.rser.2018.08.005>.
- Merlet, Y., Baviere, R., 2023. Nicolas Vasset, Optimal retrofit of district heating network to lower temperature levels. *ISSN 0360-5442 Energy Volume 282*, 128386. <https://doi.org/10.1016/j.energy.2023.128386>.
- Ministero dello Sviluppo Economico (MISE). Decreto Ministeriale 26 Giugno 2015. Applicazione 758 delle metodologie di calcolo delle prestazioni energetiche e definizione delle prescrizioni e dei requisiti minimi 759 degli edifici. *Gazzetta Ufficiale*. 2015. 760 (in Italian, available online): (www.gazzettaufficiale.it/eli/id/2015/07/15/15A05198/sg) [Accessed: 27-November-2023].
- Mugnini, A., Comodi, G., Salvi, D., Arteconi, A., 2021. Energy flexible CHP-DHN systems: unlocking the flexibility in a real plant. *Energy Convers. Manag.: X Vol. 12*, 100110. <https://doi.org/10.1016/j.ecmx.2021.100110>.
- Mugnini, A., Ferracuti, F., Lorenzetti, M., Comodi, G., Arteconi, A., 2022. Advanced control techniques for CHP-DH systems: a critical comparison of Model Predictive Control and Reinforcement Learning. *ISSN 2590-1745 Energy Convers. Manag.: X Volume 15*, 100264. <https://doi.org/10.1016/j.ecmx.2022.100264>.
- Nord, N., Nielsen, E.K.L., Kauko, H., Tereshchenko, T., 2018. Challenges and potentials for low-temperature district heating implementation in Norway. *ISSN 0360-5442 Energy Volume 151*, 889–902. <https://doi.org/10.1016/j.energy.2018.03.094>.
- International Energy Agency (IEA), Heating, 2023. Available online: www.iea.org/energy-system/buildings/heating#tracking [Accessed: 20-November-2023].
- Ochs, F., Magni, M., Dermentzis, G., 2022. Integration of heat pumps in buildings and district heating systems—evaluation on a building and energy system level. *Energies* 15, 3889. <https://doi.org/10.3390/en15113889>.
- Ommen, T., Jensen, J.K., Markussen, W.B., Reinholdt, L., Elmegaard, B., 2015. Technical and economic working domains of industrial heat pumps: part 1 – single stage vapour compression heat pumps. *ISSN 0140-7007 Int. J. Refrig. Volume 55*, 168–182. <https://doi.org/10.1016/j.jrefrig.2015.02.012>.
- Ommen, T., Markussen, W.B., Elmegaard, B., 2014. Heat pumps in combined heat and power systems. *ISSN 0360-5442 Energy Volume 76*, 989–1000. <https://doi.org/10.1016/j.energy.2014.09.016>.
- Østergaard, D.S., Svendsen, S., 2018. Experience from a practical test of low-temperature district heating for space heating in five Danish single-family houses from the 1930s. *ISSN 0360-5442 Energy Volume 159*, 569–578. <https://doi.org/10.1016/j.energy.2018.06.142>.
- Shabanpour-Haghighi, A., Seifi, A.R., 2016. Effects of district heating networks on optimal energy flow of multi-carrier systems. *Renew. Sustain. Energy Rev. Vol. 59*, 379–387. <https://doi.org/10.1016/j.rser.2015.12.349>.
- Solar Energy Laboratory, Univ. of Wisconsin-Madison, Trnsys 17 documentation: Type 31: Pipe Or Duct, Vol 4, Mathematical Reference.
- Statista. 2024. Breakdown of natural gas price for an annual average domestic consumption of 1,400 cubic meters in the regulated market in Italy from October 2022 to December 2023. Available online: www.statista.com/statistics/1339862/natural-gas-price-breakdown-for-average-domestic-consumer-italy/#:~:text=Natural%20gas%20price%20composition%20for%20domestic%20customers%20in%20Italy%20monthly%202022%2D2023&text=In%20Italy%2C%20the%20overall%20cost,an%20average%20Italian%20domestic%20consumer. [Accessed: 30-April-2024].
- Statista. 2024. Electricity price for average household consumers in Italy from 1st quarter 2017 to 1st quarter 2024. Available online: www.statista.com/statistics/792715/electricity-price-for-average-household-consumers-in-italy/ [Accessed: 30-April-2024].
- Vandermeulen, A., van der Heijde, B., Helsen, L., 2018. Controlling district heating and cooling networks to unlock flexibility: a review, 15 *Energy Vol. 151*, 103. <https://doi.org/10.1016/j.energy.2018.03.034>, 15.
- Verrilli, F., Srinivasan, S., Gambino, G., Canelli, M., Himanka, M., Del Vecchio, C., Sasso, M., Glielmo, L., 2017. Model predictive control-based optimal operations of district heating system with thermal energy storage and flexible loads. *EEE Trans. Autom. Sci. Eng. 14*, 547–557. <https://doi.org/10.1109/TASE.2016.2618948>.
- Volkova, A., Pakere, I., Murauskaitė, L., Huang, P., Lepiksaar, K., Zhang, X., 2022. 5th generation district heating and cooling (SGDHC) implementation potential in urban areas with existing district heating systems. *Energy Rep. Vol. 8*, 10037–10047. <https://doi.org/10.1016/j.egy.2022.07.162>.
- Zhang, Y., Johansson, P., Kalagasidis, A.S., 2022. Assessment of district heating and cooling systems transition with respect to future changes in demand profiles and renewable energy supplies. *Energy Convers. Manag. Vol 268*, 116038 <https://doi.org/10.1016/j.enconman.2022.116038>.